# Relationship of $Q$ Penalty to Eye-Closure Penalty for NRZ and RZ Signals With Signal-Dependent Noise

John D. Downie, *Member, OSA*

***Abstract*—The relationship between $Q$ penalty (QP) and eye-closure penalty (ECP) is examined for distorted signals in the presence of signal-dependent noise. A simple model is developed to describe the behavior of return-to-zero (RZ) modulation formats and is compared with a model for nonreturn-to-zero (NRZ) formats. The accuracy of the analysis is investigated with extensive simulations, and the numerical results from analysis and simulation are found to be in generally good agreement. Experimental measurements of distortion caused by uncompensated dispersion also show agreement with the simulation results and model predictions. The simplified models allow a means to budget QPs from distortion effects in a straightforward manner during network design for different modulation formats. The analysis predicts a smaller $Q$ penalty as a function of ECP for RZ modulation formats in comparison with NRZ and smaller relative penalties for RZ formats with narrower pulsewidths.**

***Index Terms*—Distortion, eye-closure penalty (ECP), $Q$ penalty (QP), signal-dependent noise (SDN).**

## I. Introduction

NUMERICAL simulation is an effective and well-used means of predicting the performance of optical transmission systems. It is usually based on the split-step Fourier propagation technique [1]. While accurate, this type of simulation can also be lengthy and computationally expensive with the presence of noise from optical amplifiers in the system. It is for this reason that it is sometimes desirable to obtain estimates of the effects of impairments that cause signal distortion by the relatively simple evaluation of the eye closure in the absence of noise. Signal distortion can be assessed in this manner by the simpler propagation of optical channels without noise for impairments such as fiber dispersion and without any actual distance propagation at all for some effects such as optical filtering. In fact, the effects and impairments of passage through multiple optical filters in a transparent optical network have been extensively studied with simulation and analysis in the recent past by evaluation of the eye-closure penalty (ECP) [2]–[8]. In most of these cases, the results have been either left in terms of the ECP or equated to $Q$ penalty (QP) [2] or power penalty (PP) [8] for signal-independent noise.

In general, however, the relationship between QP and ECP depends strongly on the noise statistics of the signal at the receiver. For a detected signal that is dominated by thermal noise in the photodetector, it is straightforward to show that these penalties are indeed essentially equal. However, in recent work, it has been demonstrated experimentally that for nonreturn-to-zero (NRZ) signals in the presence of signal-dependent noise (SDN) such as produced in an optically preamplified receiver, the QP is not necessarily linearly dependent on ECP and is also greater than the ECP [9], [10]. In this case, the greater signal–spontaneous beat noise of the signal "zero" values when in a distorted state (because they have a larger value than in the undistorted state) causes a larger effect to the signal $Q$ than that caused simply by a smaller eye opening. This produces a greater QP than ECP for signals with SDN, and this fact must be accounted for in estimates of the system performance when assessing the impact of impairments such as optical filtering or dispersion. This effect has been previously noted in models of the PP for distorted NRZ signals in the presence of signal-dependent noise [11]–[13].

This paper describes an investigation of the relationship between QP and ECP for signal-dependent-noise-dominated systems, which is first derived for NRZ signals with a simplified model and is then extended to return-to-zero (RZ) modulation formats. A model for RZ signals is derived based on Gaussian pulse shapes that differs significantly from the NRZ theoretical analysis. While the model developed in [8] also applied to RZ signals, it was specific to linearly chirped pulses and did not extend the results to finding the $Q$ or PP with signal-dependent noise. After the model development, computer simulation is then applied to evaluate the viability of these models for signal distortions caused by uncompensated chromatic dispersion and by spectral filtering due to passage through multiple optical filters that might represent a train of optical add–drop multiplexers (OADMs) in an optical network. Three different RZ pulse formats are studied, and we find significant agreement between the model predictions of QP and the results obtained from the simulation experiments, confirming the validity of the analysis over certain penalty ranges. Finally, experimental results are presented for both NRZ and RZ signals with distortion caused by uncompensated dispersion and compared with the models.

The remainder of this paper is divided into three sections. In Section II, the analytical expressions relating QP to ECP are derived for NRZ and RZ signal formats. The expressions are compared for different RZ formats, and a boundary for an extreme case is also determined. In Section III, the simulation experiments are described and the results presented in comparison to the analytical predictions. The laboratory experimental results are also given in this section. The work is summarized, and some conclusions drawn in Section IV.

Manuscript received August 27, 2004; revised November 23, 2004.

The author is with Corning, Inc., Science and Technology, Corning, NY 14831 USA.

Digital Object Identifier 10.1109/JLT.2005.849899

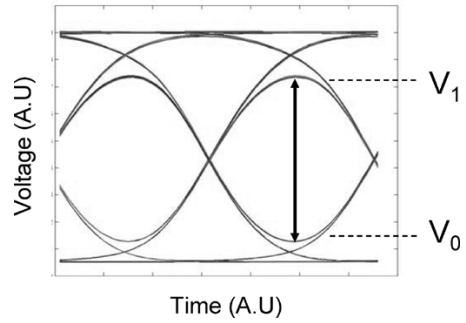


Fig. 1. Example illustration of a noiseless distorted signal electrical eye diagram and eye-closure definition.

## II. Analytical Derivation of Penalty Expressions

We begin by noting the definitions for eye closure and $Q$. The eye-closure (or eye-opening) parameter is the difference in the absence of noise between the "ones" value and the "zeros" value at the bit center, where this difference is usually maximum. This difference is defined to be between the innermost rails of the signal electrical eye diagram and is given simply as

$$\text{Eye Closure (EC)} = V_1 - V_0 \tag{1}$$

where $V_1$ is the voltage level of the minimum "ones" rail at the eye center, and $V_0$ is the voltage level of the maximum "zeros" rail. As defined in this paper, the rails in an eye diagram represent the distinct signal trajectories and voltage levels at the center of a noiseless eye, due to distortion and bit pattern dependencies. An example of a noiseless distorted eye is illustrated schematically in Fig. 1.

Within the framework of the Gaussian approximation for signal power distribution near the optimal decision level, the effective $Q$ factor is defined as

$$Q = \frac{\mu_1 - \mu_0}{\sigma_1 + \sigma_0} \tag{2}$$

where $\mu_1$ is the effective average voltage of the "ones" distribution at the eye center, $\mu_0$ is the effective average voltage of the "zeros" distribution, and $\sigma_1$ and $\sigma_0$ are the effective standard deviations of the "ones" and "zeros" distributions, respectively. These effective signal parameters are not necessarily the actual histogram values of the entire "ones" and "zeros" distributions but instead represent the values that fulfill the relationship between effective $Q$ factor and bit-error rate (BER) at the optimal decision level [14]

$$\text{BER} = \frac{1}{2}\text{erfc}\left(\frac{\text{Q}}{\sqrt{2}}\right). \tag{3}$$

It has been previously demonstrated that the statistics of the rails closest to the decision threshold level generally dominate the BER and thus $Q$ for distorted signals [15]. With this assumption, we can create a simple model of the signal distribution as if all bits have the means and standard deviations of these innermost rails. The numerator of $Q$ can therefore be regarded as being equivalent to the eye closure (EC) or $\mu_1 = V_1$ and $\mu_0 = V_0$.

The QPs and ECPs are defined as the ratios of these quantities in the absence of a distorting impairment to the quantities in the presence of the distortion. Thus, QP is expressed in general form as

$$\text{QP} = \frac{\frac{(V_{u,1}-V_{u,0})}{(\sigma_{u,1}+\sigma_{u,0})}}{\frac{(V_{d,1}-V_{d,0})}{(\sigma_{d,1}+\sigma_{d,0})}} \tag{4}$$

where the subscript "$u$" represents the undistorted state of the signal, and the subscript "$d$" represents the distorted state of the signal. An assumption underlying (4) is that the average signal powers are the same for the undistorted and distorted signal states. The ECP is written generally as

$$\text{ECP} = \frac{(V_{u,1} - V_{u,0})}{(V_{d,1} - V_{d,0})} \tag{5}$$

where it is again assumed here that the two states have equal average signal powers. QP and ECP then have the general relationship of

$$\text{QP} = \text{ECP}\frac{(\sigma_{d,1} + \sigma_{d,0})}{(\sigma_{u,1} + \sigma_{u,0})}. \tag{6}$$

Note that if the noise is independent of the signal such as for thermal detector noise, the noise variances will be identical in the undistorted and distorted states. Then, the QP simply reduces to the ECP in (6), and QP = ECP for the case of signal-independent noise, as mentioned previously. This should be true for any modulation format.

Now let us consider NRZ signals with signal-dependent noise. We follow an approach previously used to calculate the PP for distorted signals with SDN [11], [12] and apply it to calculate the QP. The approach treats signal distortion effects as if they were caused by a finite extinction ratio. The QP is defined as the ratio of the $Q$ values with infinite and finite extinction ratios. We define a finite-voltage extinction ratio corresponding to a distorted signal as

$$r = \frac{V_{d,0}}{V_{d,1}} \tag{7}$$

where $r < 1$. For the infinite extinction ratio $V_{u,0} = 0$, and thus $r = 0$. For an NRZ signal with equal probability of "ones" and "zeros," the average voltage can be reasonably approximated as

$$V_{\text{ave}} = \frac{1}{2}(V_1 + V_0). \tag{8}$$

Thus, for infinite extinction ratio (undistorted state) and finite extinction ratio (distorted state), we can write straightforward expressions as

$$V_{u,1} = 2V_{\text{ave}}, \tag{9}$$

$$V_{d,1} = \frac{2V_{\text{ave}}}{1+r} \tag{10}$$

and

$$V_{d,0} = \frac{2rV_{\text{ave}}}{1+r}. \tag{11}$$

For SDN such as signal–spontaneous beat noise caused by optical preamplification, it is well known that the variance of the noise is proportional to the optical power, and thus it is also essentially proportional to the output voltage. Using (4) and (7)–(11), we can then write the $Q$ penalty as

$$\mathrm{QP} = \frac{\frac{2V_{\mathrm{ave}}}{K\sqrt{2V_{\mathrm{ave}}}}}{\frac{\frac{2V_{\mathrm{ave}}}{(1+r)}(1-r)}{\left[K\sqrt{\frac{2V_{\mathrm{ave}}}{1+r}}+K\sqrt{\frac{2rV_{\mathrm{ave}}}{1+r}}\right]}} \tag{12}$$

where $K$ is a proportionality constant. This reduces to

$$\mathrm{QP} = \frac{(1+r)}{(1-r)} \cdot \frac{1+\sqrt{r}}{\sqrt{1+r}}. \tag{13}$$

Plugging (9)–(11) into the expression for ECP in (5), we find

$$\mathrm{ECP} = \frac{2V_{\mathrm{ave}}}{\frac{2V_{\mathrm{ave}}}{(1+r)}(1-r)} = \frac{(1+r)}{(1-r)} \tag{14}$$

and simplification produces the expression

$$\mathrm{QP} = \mathrm{ECP} \cdot \frac{1+\sqrt{\frac{(\mathrm{ECP}-1)}{(\mathrm{ECP}+1)}}}{\sqrt{1+\frac{(\mathrm{ECP}-1)}{(\mathrm{ECP}+1)}}} \tag{15}$$

as the relationship between ECP and QP for NRZ signals in the presence of signal-dependent noise. In principle, this relationship strictly holds for the penalty caused by finite extinction ratio but is an approximation for NRZ signal distortion caused by other means, as was pointed out in [12] for the related PP expression. The validity of the expression for general distortion primarily rests on the assumption that the eye is closed symmetrically from the top and bottom. It is also noted that (15) here can be related to [12, eq.(2)] by recognizing that for SDN, the $\mathrm{PP} = \mathrm{QP}^2$ in linear units and the ECP in (15) is the same as the PP for signal-independent noise (SIN). The relationship between PP and QP also allows us to equate any results for QP expressed in 20log() format to the PP, or equivalently, the optical-signal-to-noise ratio (OSNR) penalty, expressed in the conventional 10log() format. Equation (15) will be presented in graphical form along with an analogous expression for RZ formats later in the paper.

For RZ modulation formats, a slightly different approach is taken to estimating the QP as a function of ECP for signals with SDN. In this case, we treat RZ signal pulses as Gaussian functions and make the assumption that the pulse in the distorted state is still Gaussian shaped, but with wider pulsewidth and lower peak power than in the undistorted state. This is, of course, a somewhat oversimplified approximation to general signal distortion caused by impairments such as dispersion and spectral filtering. Under this assumption and that of equal pulse energies, we can express the functional forms of the undistorted and distorted RZ voltage pulses as

$$V_u(t) = \frac{\gamma}{T_u}\exp\left[-\left(\frac{t}{T_u}\right)^2\right] \tag{16}$$

and

$$V_d(t) = \frac{\gamma}{T_d}\exp\left[-\left(\frac{t}{T_d}\right)^2\right] \tag{17}$$

where $2T_u$ and $2T_d$ represent the $e^{-1}$ pulsewidths of the two pulse types, and $\gamma$ is a constant.

Now we can calculate QP and ECP using (4) and (5) for a general RZ modulation format. To begin, the pulse values of the "ones" bits at the maximum eye-opening position are taken as

$$V_{u,1} = V_u(t=0) = \frac{\gamma}{T_u} \tag{18}$$

and, similarly

$$V_{d,1} = \frac{\gamma}{T_d} \tag{19}$$

assuming that the pulse is centered at $t = 0$. The values of the "zeros" bits are approximated as

$$V_{u,0} = 2 \cdot V_u(t=T_B) = 2\frac{\gamma}{T_u}\exp\left[-\left(\frac{T_B}{T_u}\right)^2\right] \tag{20}$$

and

$$V_{d,0} = 2\frac{\gamma}{T_d}\exp\left[-\left(\frac{T_B}{T_d}\right)^2\right] \tag{21}$$

where $T_B$ represents a bit period. The coefficient of 2 in front of the expressions for $V_{u,0}$ and $V_{d,0}$ reflects the assumption that the maximum "zeros" rail at the eye-opening position results from the bit sequence 101, i.e., where the zero is surrounded by "ones" pulses. In this case, we might reasonably expect the value of the "zero" to be the addition of the Gaussian pulse values from both sides. By substituting (18)–(21) into (5), we calculate ECP as

$$\mathrm{ECP} = \frac{T_d}{T_u}\left[\frac{1-2\exp\left[-\left(\frac{T_B}{T_u}\right)^2\right]}{1-2\exp\left[-\left(\frac{T_B}{T_d}\right)^2\right]}\right]. \tag{22}$$

Similarly, the $Q$ penalty can be expressed from (6) as

$$\mathrm{QP} = \mathrm{ECP} \cdot \frac{\left(K\sqrt{\frac{\gamma}{T_d}}+K\sqrt{2\left(\frac{\gamma}{T_d}\right)\exp\left[-\left(\frac{T_B}{T_d}\right)^2\right]}\right)}{\left(K\sqrt{\frac{\gamma}{T_u}}+K\sqrt{2\left(\frac{\gamma}{T_u}\right)\exp\left[-\left(\frac{T_B}{T_u}\right)^2\right]}\right)} \tag{23}$$

and finally

$$\mathrm{QP} = \frac{\mathrm{ECP}}{\sqrt{\frac{T_d}{T_u}}} \cdot \frac{\left(1+\sqrt{2}\cdot\exp\left[\frac{-\left(\frac{T_B}{T_d}\right)^2}{2}\right]\right)}{\left(1+\sqrt{2}\cdot\exp\left[\frac{-\left(\frac{T_B}{T_u}\right)^2}{2}\right]\right)}. \tag{24}$$

In (22) and (24), $T_u$ is a constant that describes the undistorted pulsewidth, while $T_d$ is the distorted pulsewidth parameter whose value dictates the eye-closure and $Q$ penalties.

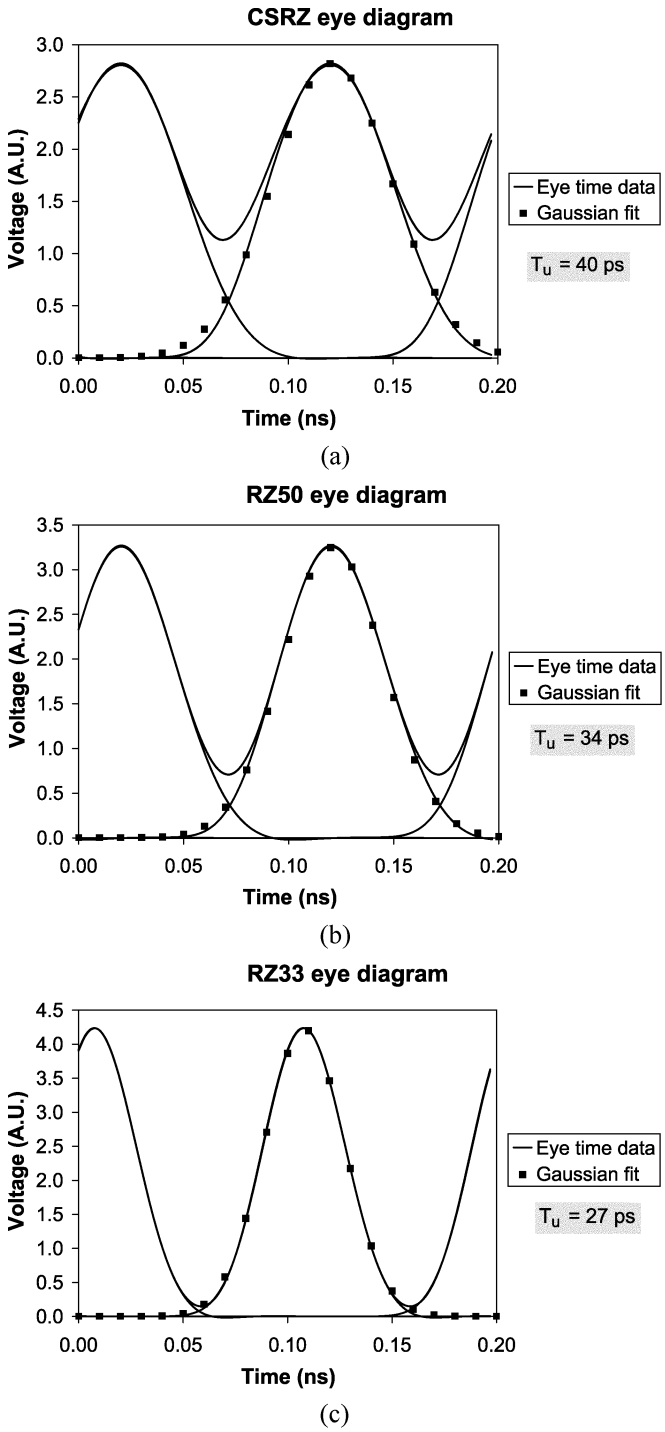


Fig. 2. Noiseless electrical eye diagrams of (a) CSRZ, (b) RZ50, and (c) RZ33 modulation formats in an optical back-to-back condition with discrete points representing the best Gaussian fits to each pulse shape.

Before continuing, we consider the extreme RZ case that sets a lower boundary to the function of QP as a function of ECP. Consider an RZ format with a pulsewidth narrow enough (short enough duty cycle) such that the "zero"'s value at the eye-opening location for both the undistorted and distorted states of the signal is approximately zero. That is, we assume that

$$V_{d,0} = V_{u,0} \approx 0 \tag{25}$$

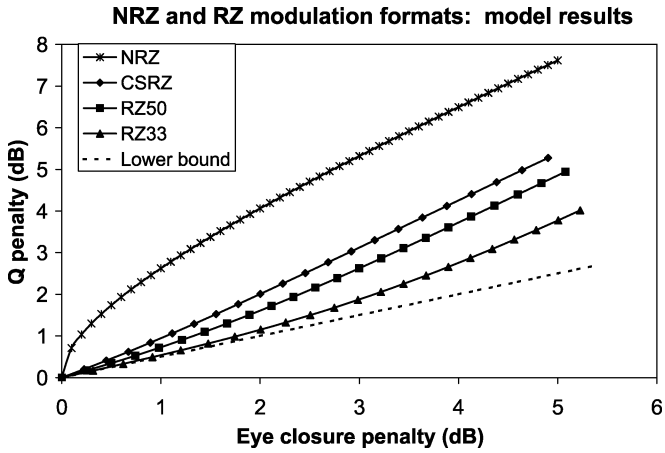


Fig. 3. Model results for QP as a function of ECP.

implying that the signal distortion is manifested through the "one"'s value without appreciably changing the "zero"'s In this case, the ECP is given simply as

$$\text{ECP} = \frac{V_{u,1}}{V_{d,1}} = \frac{T_d}{T_u} \tag{26}$$

and the QP then becomes

$$\text{QP} = \text{ECP} \cdot \frac{\sigma_{d,1}}{\sigma_{u,1}} = \text{ECP} \cdot \frac{\sqrt{T_u}}{\sqrt{T_d}}. \tag{27}$$

Combining (26) and (27), we then see that in this extreme case the QP is related to the ECP as

$$\text{QP} = \sqrt{\text{ECP}} \tag{28}$$

or expressed in units of decibel

$$\text{QP}\,(\text{dB}) = \frac{1}{2}\text{ECP}\,(\text{dB}). \tag{29}$$

In this case, a QP of 0.5 dB results from each decibel of ECP if both penalties in decibel units are calculated with the same coefficient in front of the logarithm. For general RZ signals, the relationship between QP and ECP as expressed by (22) and (24) ensures a QP dependence larger than the extreme case, or lower bound.

To gain an understanding of the RZ model results given in (22) and (24), we consider three different types of RZ modulation formats. The three formats are carrier-suppressed RZ (CSRZ), 50% duty cycle RZ (RZ50), and 33% duty cycle RZ (RZ33). To determine the Gaussian parameter $T_u$ that best describes these formats, a 10-Gb/s signal of each type was generated within a optical system simulation tool. The electrical eye time-domain data for each was captured in an optical back-to-back condition with no noise, and a Gaussian function as described by (16) was fit to the eye diagram. The electrical filters used in the receiver in the simulations were fifth-order Bessel functions with bandwidths of 8 GHz for the CSRZ and RZ50 signals and 11 GHz for the RZ33 signal. The three RZ format eye diagrams with accompanying data points representing the best Gaussian fit are shown in Fig. 2. For a 10-Gb/s signal bit

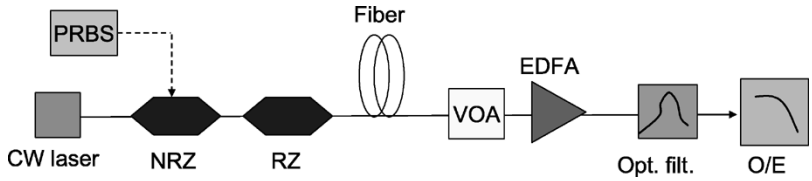


Fig. 4. Simulation experiment setup to measure $Q$ results as a function of uncompensated fiber dispersion.

rate, the $T_u$ pulsewidth values found by the fitting process for CSRZ, RZ50, and RZ33 were 40, 34, and 27 ps, respectively.

The relationships between QP and ECP for each of the three RZ formats can be determined according to the simple model described previously by (22) and (24), as parameterized by the distorted pulsewidth $T_d$. As discussed previously, the values of $T_u$ were determined by fitting Gaussian functions to the undistorted pulse shapes. The parameter $T_d$ was then varied with $T_d \geq T_u$, and ECP and QP were calculated. The QP is shown as a function of the ECP in Fig. 3 for the three RZ formats. Also shown in the figure is the QP function for the NRZ format as given in (15), and the lower bound for the RZ formats described by (29). The results show that all three RZ formats have a significantly weaker dependence of QP on ECP than the NRZ format. Consistent with this, RZ formats with a larger duty cycle show a stronger dependence on ECP than shorter duty cycle formats. Thus, for a given eye-closure value, CSRZ has a greater QP than RZ50, which in turn has a greater QP than RZ33. We also note that the QP function for RZ33 is very close to the theoretical lower bound for smaller values of ECP less than 2 dB or so. The data in Fig. 3 are shown in units of decibels in 20log() format for both QP and ECP.

## III. Simulation and Laboratory Experiments and Results

### A. Simulations and Results

In order to explore the validity of the model results shown in Fig. 3, a series of simulation experiments were conducted with an optical fiber communication system modeling tool. Two different impairments were studied that cause signal distortion: 1) chromatic dispersion and 2) spectral filtering from passage through multiple optical filters. For each impairment type, simulations were performed with all three RZ modulation formats as well as NRZ. $Q$ data was collected for the systems with three different nominal OSNR values by use of the $Q$ calculation function in the modeling tool. ECP data were collected by transmission of the signals through identical systems without noise, and the electrical eye data was analyzed to calculate the ECP. A schematic diagram of the optical system set up in the simulation environment to model the performance as a function of dispersion is shown in Fig. 4.

As shown in the figure, the transmitter consisted of a continuous-wave (CW) laser at wavelength 1550 nm, a pseudorandom bit sequence (PRBS) generator, and two Mach–Zehnder (MZ) modulators for RZ signals (one modulator for NRZ signals). The first MZ modulator was modulated in NRZ format with the PRBS pattern at a bit rate of 10 Gb/s, while the second MZ device was sinusoidally driven and carved out the RZ pulses of interest. Three different RZ pulse types were studied: CSRZ, RZ50, and RZ33. The RZ signal was propagated through a piece of fiber to produce a given state of dispersion. The fiber had a dispersion parameter $D = 100$ ps/nm/km. Nonlinear effects were precluded by low channel launch powers ($<$0 dBm) and the short fiber lengths required ($\leq$14 km). The signal was then passed through a variable optical attenuator (VOA) and erbium-doped fiber amplifier (EDFA) with the VOA set to control the OSNR of the signal. The receiver was represented by an optical filter and optical-to-electrical (O/E) conversion with a given electrical filter bandwidth. The optical filter was a fourth-order Butterworth filter with 40-GHz 3-dB bandwidth. The electrical filters used were the same as described previously for the RZ signals, and the electrical filter for NRZ signals was also a fifth-order Bessel filter with 8.0-GHz bandwidth. The length of the PRBS used in the $Q$ measurements was 4096 b. Signal OSNR values of 20, 23, and 26 dB were investigated. Uncompensated accumulated fiber dispersion values of 0 to 900 ps/nm were simulated in the experiments by varying the length of the fiber for RZ signals, and up to 1400 ps/nm for NRZ signals. The simulation tool used is a general optical system modeling tool that employs a conventional split-step Fourier method for signal propagation [1] and optical and electrical filtering applied in the frequency domain.

The $Q$ calculation used in the modeling tool essentially determines the means and standard deviations of the signal power for the "ones" and "zeros" in the bit sequence and implicitly assumes Gaussian noise statistics. A pattern dependence feature was employed in the calculations that effectively recognizes the rail structure of the eye and calculates a $Q$ value that is a weighted average of the $Q$ values determined from the different rails. This approach using patterning effects more closely reflects the measurement of $Q$ in a laboratory experiment where $Q$ is determined from BER measurements in the Gaussian tails of the signal distribution and is also generally consistent with our modeling assumption that the innermost rails dominate the BER and $Q$ values at the optimal decision threshold. We will discuss implications of this assumption subsequently.

The setup used to calculate the ECP was identical to that shown in Fig. 4, except that the EDFA was removed. The signal was noiseless in this case. The definitions of the optical filter and the electrical filter in the O/E converter for ECP data were the same as those used in the $Q$ probe when measuring $Q$ data. The PRBS length used when generating the ECP data with the electrical eye probe was 512 b. The ECP was calculated with reference to the eye of a back-to-back system and normalized to eliminate any contribution from simple signal loss. This ensures the ECP calculated was due to the signal distortion alone.

The second signal distortion impairment studied here was spectral filtering produced by passage of the signal through a series of optical filters that might represent a series of OADM

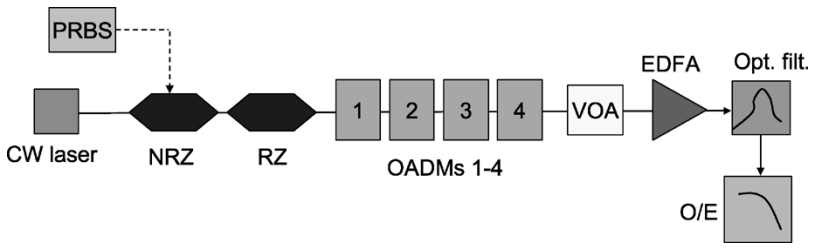


Fig. 5. Simulation experimental setup to measure $Q$ results as a function of spectral filtering induced distortion.

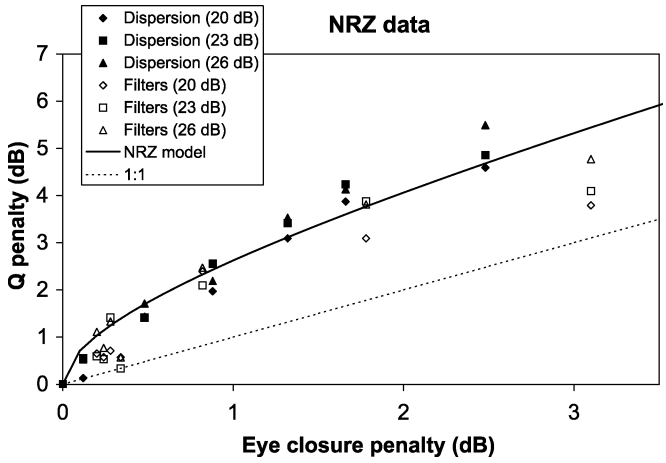


Fig. 6. Simulation experiment results and analytical prediction for QP as a function of ECP for an NRZ modulation format. The dashed line represents a 1:1 penalty relation.

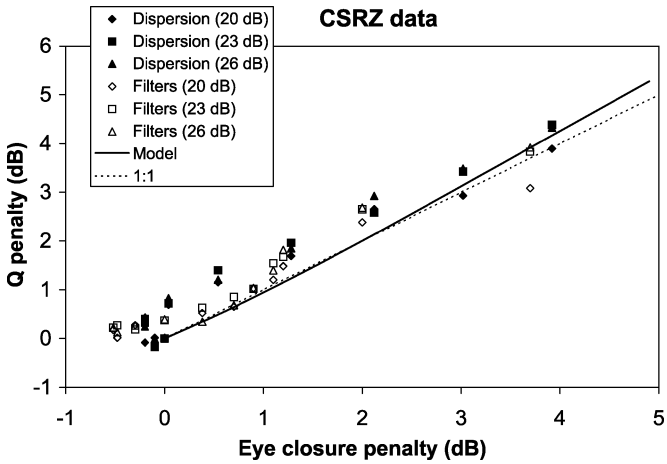


Fig. 7. Simulation experiment results and analytical prediction for QP as a function of ECP for CSRZ modulation format. The dashed line represents a 1:1 penalty relation.

devices. The signal passed through four OADMs, each of which contained two optical filters. The optical filters were complex fourth-order Butterworth filters (amplitude and phase) with 3-dB bandwidths of 40 GHz. The amount of distortion or penalty induced was controlled by varying the wavelength of the laser, which was tuned across the passband of the optical filters in the OADMs. The OADM filters were centered at 1550 nm. As before, the PRBS length used to calculate $Q$ data was 4096 b, and data was collected for OSNR values of 20, 23, and 26 dB. Again, the VOA was used to control the signal power into the EDFA and thus the signal OSNR value. A schematic diagram of the optical system in the simulation tool used to generate data with the filtering-induced distortion is shown in Fig. 5. The ECP data was again taken for a noiseless system in which the amplifier was removed, and the number of bits in the PRBS used to generate the ECP data was 512.

The first modulation format studied is NRZ. Previous laboratory experiments involving filter concatenation distortion by passage through 50-GHz OADMs have indirectly supported the accuracy of (15) as it was determined that the relationship expressed in (15) was required to explain the measured QP data [9], [10]. Direct simulation results are shown first here, and direct experimental results will be presented subsequently. The NRZ simulation systems were identical to those shown in Figs. 4 and 5 except that the second MZ modulator that creates RZ pulses was removed. QP versus ECP results from the dispersion and optical filtering simulation experiments are shown in Fig. 6, along with the model results of (15), and a 1:1 penalty relation. We see a generally good fit of the simulation data to the model prediction. In the figure, the data symbols are described by the impairment type with the OSNR value in parenthesis. According to this data, there is not a highly significant dependence on OSNR, although for larger penalty values, the results do suggest slightly lower QPs for lower OSNR values. The results also suggest that the model may somewhat overestimate the QP for larger values of ECP. The principle explanation for this is likely that the assumption of symmetry in the eye closing is less accurate for large distortions. The dependence of the PP (or QP) on the eye-closure symmetry has been previously explored and discussed by Rebola and Cartaxo [13]. Another smaller reason may be that our simple model does not account for the actual probability of occurrence of the innermost rail levels [15] but assumes that all bits have power values corresponding to those rails. This source of error, while generally small, should be more important for larger penalties, which is in qualitative agreement with the observed behavior. Together, the lack of symmetric eye closing and accounting for the probability of rail occurrence appear to suggest that the NRZ model prediction is most accurate for ECP values $<3$ dB in 20 log (ECP) format.

The simulation results along with model predictions are presented in Figs. 7–9 for the CSRZ, RZ50, and RZ33 modulation formats. These results also show significant agreement between the simulation data and the analytical predictions of (22) and (24). Even though the Gaussian model developed for RZ formats is clearly an approximation to the behavior of real distortions, the ability of the model to predict the dependence of QP in the presence of signal-dependent noise on ECP in a noiseless system is reasonably good. The models for NRZ and RZ formats

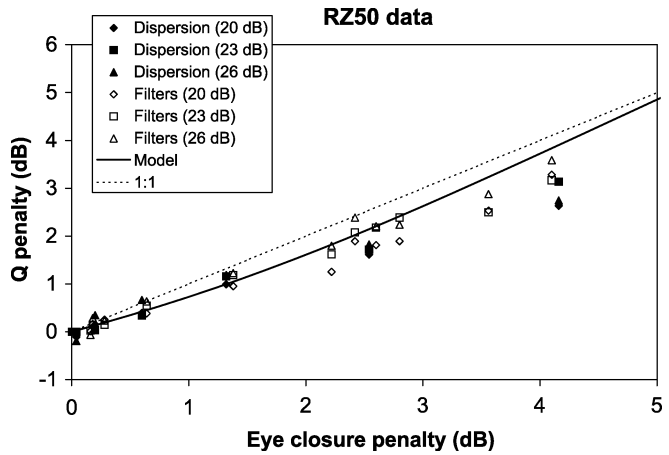


Fig. 8. Simulation experiment results and analytical prediction for QP as a function of ECP for RZ50 modulation format. The dashed line represents a 1:1 penalty relation.

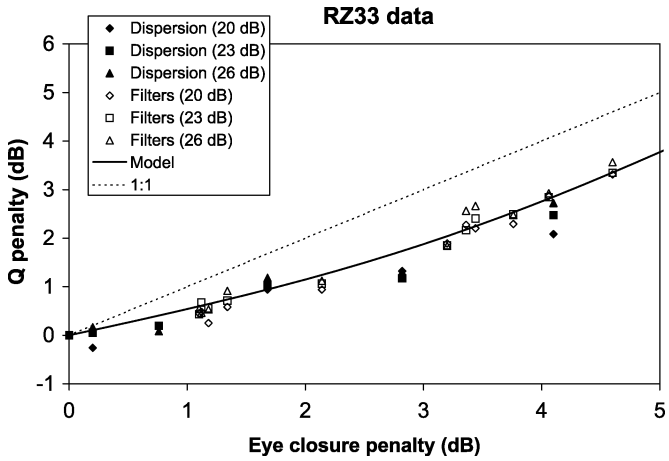


Fig. 9. Simulation experiment results and analytical prediction for QP as a function of ECP for RZ33 modulation format. The dashed line represents a 1:1 penalty relation.

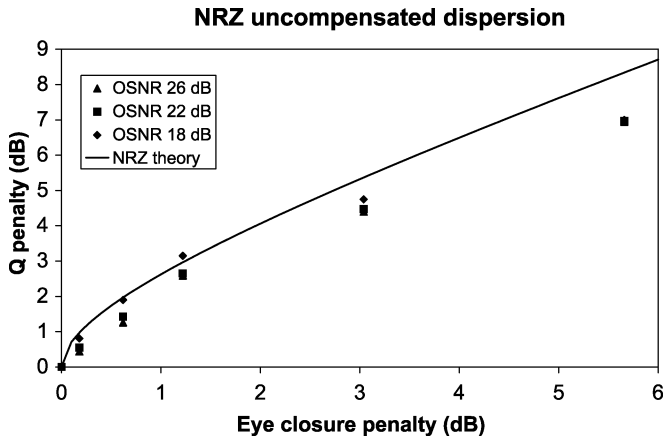


Fig. 10. Experimental results with model prediction for QP and a function of ECP for an NRZ signal.

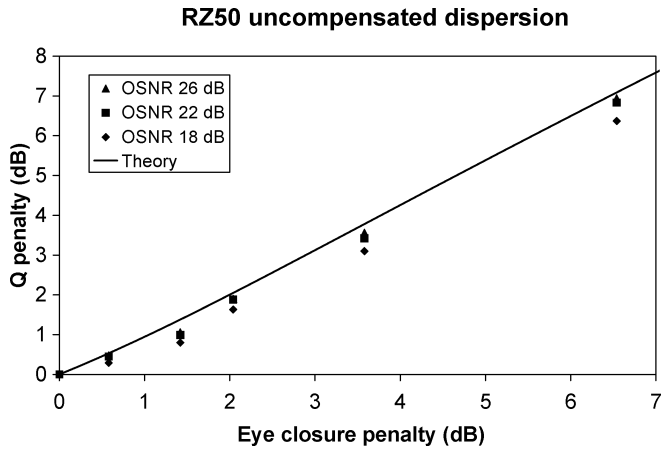


Fig. 11. Experimental results with model prediction for QP and a function of ECP for an RZ50 signal.

allow quick estimation of the QP for signal distortions that can be characterized by ECPs. We note that the dependence of QP on ECP is nearly 1:1 for the simulated CSRZ signal, while the RZ50 and RZ33 models and simulation data predict smaller QPs than ECPs. As noted for the NRZ results, an improvement to the simple model described in this paper would be to account for the probability of the rail occurrence. Without this accounting, the model probably slightly overestimates the QP for large values of the ECP. However, we note that the amount of this overestimation is dependent on the absolute $Q$ value—and, therefore, on the OSNR and any other nonlinear penalties that signal may suffer—and would not be simple to include in a general way. Given its expected small effect and the good agreement of the simulation results, the simple model presented here appears to be accurate over a fairly large range of penalty values.

### *B. Laboratory Experimental Results*

To complement the simulation results and confirm their validity, laboratory experiments were conducted with signal distortions produced by uncompensated dispersion for NRZ and RZ50 signals. The laboratory experimental setup was very similar to that shown in Fig. 4, with the electrical signal passed to a BER tester (BERT) to perform $Q$ measurements based on BER data as a function of decision threshold [14]. The PRBS employed was of length $2^{31} - 1$. The RZ50 modulator in the setup was driven with a sine wave at the clock frequency of 10 Gb/s. The transfer function of the O/E and radio-frequency (RF) amplifier used in the setup was measured with a network analyzer. This transfer function was fit fairly well by a fourth-order Bessel function with 3-dB bandwidth of 6 GHz, and this Bessel function electrical filter was then used in the noiseless simulation of the system in which the ECP was calculated as a function of the accumulated fiber dispersion. For the RZ50 signal, the 6-GHz fourth-order Bessel function was found in simulation to produce a Gaussian pulse shape with the undistorted pulsewidth parameter $T_u = 40$ ps. Note that this pulsewidth is the same as was used in the previous simulations for the CSRZ signal. However, recall that the electrical filters employed in the simulation experiments were fifth-order Bessel functions with 8-GHz bandwidth, and it is the narrower bandwidth of the experimental electrical filter transfer function that produces the same pulsewidth for the RZ50 signal.

As with the simulations, the experimental $Q$ values were measured for three different OSNR values as a function of uncompensated dispersion. The OSNR was controlled by the VOA that regulated the signal power level into the receiver preamplifier. For both the NRZ and RZ experimental signals, the launch power was $\sim$0 dBm so there were no significant nonlinear impairments in the system. The eye-closure values were calculated from noiseless simulations using the electrical filter as just described. The QP measurements as a function of the ECP calculations are shown for both NRZ and RZ50 signals in Figs. 10 and 11, respectively. The behavior of the experiment data clearly is quite similar to the previous simulation data and largely agrees with the model predictions. As mentioned previously, the overestimation of QP for ECP $>$ 3 dB for the NRZ signal is probably predominantly due to the lack of accuracy of the symmetry assumption of the eye closure. Both QP and ECP are presented in 20log() format for the experimental results.

## IV. Summary

In this paper, we have investigated the relationship between $Q$ penalty (QP) and eye-closure penalty (ECP) for nonreturn-to-zero (NRZ) and return-to-zero (RZ) modulation formats in the presence of signal-dependent noise such as is characteristic of optically preamplified receivers. Theoretical expressions relating QP and ECP were derived based on simplified models. For NRZ signals, the model assumed that signal distortion can be treated in a similar way to finite extinction ratio. For RZ signals, pulses are modeled as Gaussian functions and a very simple approach treats distorted signals as wider Gaussians than the original undistorted pulse. The resulting relationship between QP and ECP is parameterized by a distorted pulsewidth. The modeling analysis predicts significantly weaker functional dependences of the QP on ECP for RZ signals than for NRZ. Furthermore, shorter duty-cycle RZ signals are predicted to have a smaller QP for a given ECP level than larger duty-cycle RZ signals. Note that this does not mean that shorter duty-cycle RZ signals have smaller penalties for a given dispersion value, for example, but smaller QPs for a given ECP. In the extreme, a lower bound for the relationship for a short duty-cycle RZ format is $\mathrm{QP(dB)} = 0.5\ \mathrm{ECP(dB)}$, where both QP and ECP expressed in decibels have the same multiplying coefficient (i.e., 20log(QP), 20 log(ECP)).

Simulation and laboratory experiments designed to test the model predictions showed generally good agreement with the analytical results for both NRZ and RZ modulation formats. Overall, the Gaussian model for RZ signals shows a reasonably good ability to predict QP as a function of ECP in the presence of signal-dependent noise, even though it is a simple approximation. This model, and that of the NRZ signals, allows quick and easy estimation of expected QPs in systems for impairments that can be described and calculated as an ECP. Thus, the system level effects of impairments such as dispersion and filter-induced distortion may be more accurately predicted by noiseless simulation and the calculated ECP converted to a QP estimate. Of course, for filter concatenation penalties, there may be other effects that also need to be included in a complete analysis, such as OSNR penalty across the filter passband caused by amplified spontaneous emission noise shaping [9], [10], [13]. The analysis presented here focused only on capturing the effects of the signal distortion.

## References


[1] G. P. Agrawal, *Nonlinear Fiber Optics*, 2nd ed. San Diego, CA: Academic, 1995.

[2] J. D. Downie and A. B. Ruffin, "Analysis of signal distortion and crosstalk penalties induced by optical filters in optical networks," *J. Lightw. Technol.*, vol. 21, no. 9, pp. 1876–1886, Sep. 2003.

[3] J. D. Downie, I. Tomkos, N. Antoniades, and A. Boskovic, "Effects of filter concatenation for directly modulated transmission lasers at 2.5 and 10 Gb/s," *J. Lightw. Technol.*, vol. 20, no. 2, pp. 218–228, Feb. 2002.

[4] N. N. Khrais, A. F. Elrefaie, R. E. Wagner, and S. Ahmed, "Performance of cascaded misaligned optical (de)multiplexers in multiwavelength optical networks," *IEEE Photon. Technol. Lett.*, vol. 8, no. 8, pp. 1073–1075, Aug. 1996.

[5] N. N. Khrais, A. F. Elrefaie, and R. E. Wagner, "Performance degradations of WDM systems due to laser and optical filter misalignments," *Electron. Lett.*, vol. 31, pp. 1179–1180, Jul. 1995.

[6] N. N. Khrais, A. F. Elrefaie, R. E. Wagner, and S. Ahmed, "Performance degradation of multiwavelength optical networks due to laser and (de)multiplexer misalignments," *IEEE Photon. Technol. Lett.*, vol. 7, no. 11, pp. 1348–1350, Nov. 1995.

[7] T. Otani, N. Antoniades, I. Roudas, and T. E. Stern, "Cascadability of passband-flattened arrayed waveguide-grating filters in WDM optical networks," *IEEE Photon. Technol. Lett.*, vol. 11, no. 11, pp. 1414–1416, Nov. 1999.

[8] K.-P. Ho, L.-K. Chen, and F. Tong, "Modeling of waveform distortion due to optical filtering," *IEEE J. Sel. Topics Quantum Electron.*, vol. 6, no. 2, pp. 223–226, Mar.–Apr. 2000.

[9] J. D. Downie, F. Annunziata, J. Hurley, and J. Amin, "Relative contributions to filter-induced Q penalty from eye closure and OSNR degradation," presented at the Optical Fiber Communications Conf. 2004, Los Angeles, CA, Feb. 22–27, 2004, Paper ThT4.

[10] ——, "Fixed low channel-count OADM filter concatenation experiments with 50 GHz channel spacing and 10 Gb/s NRZ signals," *J. Opt. Netw.*, vol. 3, pp. 204–213, 2004.

[11] M. Kuznetsov, N. M. Froberg, S. R. Henion, and K. A. Rauschenbach, "Power penalty for optical signals due to dispersion slope in WDM filter cascades," *IEEE Photon. Technol. Lett.*, vol. 11, no. 11, pp. 1411–1413, Nov. 1999.

[12] M. Kuznetsov, N. M. Froberg, S. R. Henion, C. Reinke, and C. Fennelly, "Dispersion-induced power penalty in fiber-Bragg-grating WDM filter cascades using optically preamplified and nonpreamplified receivers," *IEEE Photon. Technol. Lett.*, vol. 12, no. 10, pp. 1406–1408, Oct. 2000.

[13] J. L. Rebola and A. V. T. Cartaxo, "Power penalty assessment in optically preamplified receivers with arbitrary optical filtering and signal-dependent noise dominance," *J. Lightw. Technol.*, vol. 20, no. 3, pp. 401–408, Mar. 2002.

[14] N. S. Bergano, F. W. Kerfoot, and C. R. Davidson, "Margin measurements in optical amplifier systems," *IEEE Photon. Tech. Lett.*, vol. 5, no. 3, pp. 304–306, Mar. 1993.

[15] S. Norimatsu and M. Maruoka, "Accurate $Q$-factor estimation of optically amplified systems in the presence of waveform distortion," *J. Lightw. Technol.*, vol. 20, no. 1, pp. 19–27, Jan. 2002.



**John D. Downie** received the Bachelor's degree in optics with highest honors from the University of Rochester, Rochester, NY, in 1983; the Certificate of Post-Graduate Study in physics from Cambridge University, Cambridge, U.K., in 1984; and the Ph.D. degree in electrical engineering from Stanford University, Stanford, CA, in 1989.

In 1989, he joined the National Aeronautics and Space Administration (NASA) Ames Research Center, where he was a Research Scientist and Group Leader of the Information Physics Research Group, conducting research in optical information processing and optical data storage. He joined Corning, Incorporated, Corning, NY, in 1999 as a Research Associate in the Science and Technology Division, where his current research interests center on optical fiber communications and networking. His work at Corning has included optical performance monitoring, the effects of filter concatenation in long-reach transparent networks, optical crosstalk in networks, issues of metro optical transport, dispersion management in optical networks, modeling of device and system performance, advanced modulation formats, and experimental systems research at 10 and 40 Gb/s. He has published more than 70 peer-reviewed journal papers and conference publications.

Dr. Downie is a Member of the Optical Society of America (OSA). He was awarded the Churchill Foundation Scholarship to study at Cambridge University.